

PROCEEDINGS OF SPIE

[SPIDigitalLibrary.org/conference-proceedings-of-spie](https://spiedigitallibrary.org/conference-proceedings-of-spie)

In-line characterization of non-selective SiGe nodule defects with scatterometry enabled by machine learning

Dexin Kong, Robin Chao, Mary Breton, Chi-chun Liu, Gangadhara Raja Muthinti, et al.

Dexin Kong, Robin Chao, Mary Breton, Chi-chun Liu, Gangadhara Raja Muthinti, Soon-cheon Seo, Nicolas J. Loubet, Pietro Montanini, John Gaudiello, Veeraraghavan Basker, Aron Cepler, Susan Ng-Emans, Matthew Sendelbach, Itzik Kaplan, Gilad Barak, Daniel Schmidt, Julien Frougier, "In-line characterization of non-selective SiGe nodule defects with scatterometry enabled by machine learning," Proc. SPIE 10585, Metrology, Inspection, and Process Control for Microlithography XXXII, 1058510 (5 September 2018); doi: 10.1117/12.2297377

SPIE.

Event: SPIE Advanced Lithography, 2018, San Jose, California, United States

In-line characterization of non-selective SiGe nodule defects with scatterometry enabled by machine learning

Dexin Kong ^a, Robin Chao ^a, Mary Breton ^a, Chi-chun Liu ^a, Gangadhara Raja Muthinti ^a,
Soon-cheon Seo ^a, Nicolas J. Loubet ^a, Pietro Montanini ^a, John Gaudiello ^a, Veeraraghavan
Basker ^a, Aron Cepler ^b, Susan Emans ^b, Matthew Sendelbach ^b, Itzik Kaplan ^c, Gilad Barak ^c,
Michael Shifrin ^c, Daniel Schmidt ^d, Julien Frougier ^d

^a IBM, 257 Fuller Road, Albany, NY, 12203

^b Nova Measuring Instruments, Inc., 3090 Oakmead Village Drive, Santa Clara, CA 95051, USA

^c Nova Measuring Instruments, LTD, P.O. Box 266, Weizmann Science Park, Rehovot 76100, Israel

^d GLOBALFOUNDRIES, 400 Stone Break Rd Extension, Malta, NY 12020

ABSTRACT

As device scaling continues, defects related to the nucleation of non-epitaxial SiGe, in the form of nodules, are becoming more problematic. These are generated during the source/drain epitaxial growth process and are difficult to control and measure. In this work, novel methods, based on scatterometry and machine learning, are developed to accurately and comprehensively measure the SiGe nodules. The results of scatterometry-based defect measurements are compared to top-down scanning electron microscopy (SEM), cross-sectional SEM and transmission electron microscopy (TEM). With the advances in the scatterometry-based defect measurement metrology, we demonstrate such fast, quantitative, and comprehensive measurement of SiGe nodule defects can be used to improve the metrology throughput and device yield.

Keywords: Scatterometry, gate all around, nodules, machine learning

1. INTRODUCTION

Novel architectures are under development for beyond 7nm node technology, including Gate All Around (GAA) nanosheet (NS) field effect transistor (FET) [1,2,3,4]. This architecture is much more complicated than traditional FinFET structures, with many more degrees of freedom that must be controlled. The combination of the shrinking of the device size and complicated structure make it very challenging for comprehensive defect inspection techniques. Therefore, the development of advanced defect inspection techniques, with comprehensive defect characterization and high throughput, is a key part of enablement of the novel architectures.

In this paper, we propose a novel defect characterization technique for one specific type of defect, non-selective SiGe nodules. The typical morphology of SiGe nodule defects is shown in Fig. 1, which shows both top-down scanning electron microscopy (SEM) and tilted cross-sectional SEM images. The SiGe nodule defects are formed during SiGe epitaxy (EPI) growth for p-type FET source and drain (S/D). The process window for SiGe EPI growth with low nodule density becomes extremely tight due to the shrinking of contact poly pitch (CPP) and complicated NS FET structure. Any tiny process shift or incoming structure shift could introduce high densities of nodule defects, which could affect device performance and yield. The current defect inspection technique (in-line electron-beam inspection) is limited by low throughput and can only provide limited and semi-qualitative information about nodule defects, so a fast and quantitative characterization technique is preferred for measuring and monitoring this type of defect.

The proposed novel defect characterization method is based on scatterometry, because it is a fast and non-destructive in-line metrology. It is known that scatterometry is typically used for critical dimension measurement of periodic structures, also known as optical critical dimension (OCD). However, the SiGe nodule defects are random and irregular structures, which are difficult to account for in a model which is forced to be periodic. Therefore, machine learning (ML) algorithms are employed in conjunction with OCD to characterize the nodule defects. Machine learning methods can be used to create

a direct link between the scatterometry spectra and the SiGe nodule defect density/size. It will be demonstrated that our novel defect-characterization methods can help to characterize the vertical locations of nodule defects. Additionally, this technique can help to identify correlations between nodule defects and device structural parameters, which cannot be measured with any of current in-line defect inspection techniques.

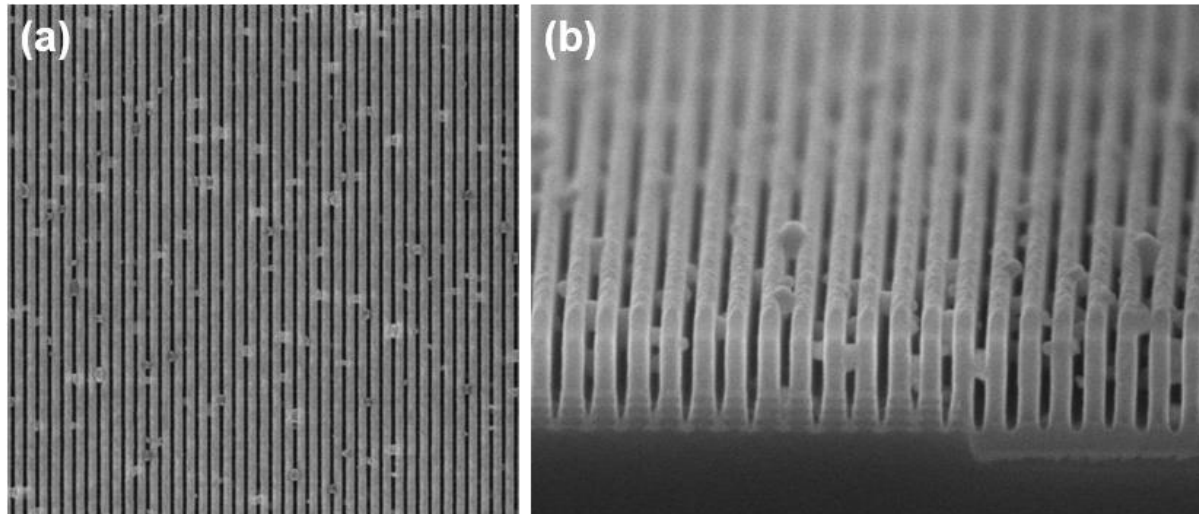


Figure 1: Typical morphologies of SiGe nodule defects. (a) top-down SEM image, (b) tilted cross-sectional SEM image which shows that SiGe nodule defects are not necessarily always on the top surface and that significant amount of nodule defects are in between the poly gates.

The vertical location of SiGe nodule defects is related to the device failure, because tungsten cannot form good contact with S/D if the nodules are at the bottom or the middle along the gate. Therefore, understanding the vertical location of nodule defects is needed to improve the device yield. The information about correlation between nodule defects and structural parameters provides important feedback for EPI process engineers to optimize EPI growth. With the advances in the scatterometry-based defect measurement metrology, we demonstrated the fast, quantitative, and comprehensive measurement of SiGe nodule defect could improve the throughput and yield. The same principle is believed to be able to apply to other types of defects.

2. DESIGN OF EXPERIMENTS (DOE)

In this work, two NS FET wafers are used for developing the novel scatterometry-based defect characterization methods. One wafer was processed with the process of record (POR) recipe (with the goal of having as few nodules as possible), and the other wafer was processed with a different recipe in order to intentionally introduce higher density of SiGe nodule defects. The NS structure we investigated has contact poly pitch (CPP) of 44 nm.

Both wafers were measured after the SiGe EPI growth processing step with in-line scatterometry and critical dimension scanning electron microscopy (CDSEM). After all necessary in-line measurements, they were cleaved in order to acquire cross-sectional images. The cross-sectional images are needed to help confirm the ability of our novel methods to accurately capture the vertical location of the nodules. Each of the in-line metrologies and ML will be described in this section.

2.1 Scatterometry

Scatterometry is a very common ‘workhorse’ metrology tool, used for fast and non-destructive measurement of geometrical and material parameters. Fig. 2 shows a schematic explaining the operation of scatterometry. The wafers are measured in the scatterometry tool for raw spectra collection. A scatterometry model then interprets the raw spectra. The

dimensional and material information can be retrieved by fitting spectra to the model. The model can be further improved by comparing to a reference such as transmission electron microscopy (TEM) before installing the model on the tool. Once the model is installed on the tool, the scatterometry measurement for the specific step can be activated for in-line measurement with high throughput. When working with scatterometry, the user must account for the time needed to build a model, and the resources needed to enable a comparison to a reference, such as TEM or CDSEM. Additionally, in the case of a significant process change or material change, the scatterometry model may need to be updated with additional reference metrology and model rebuilding time.

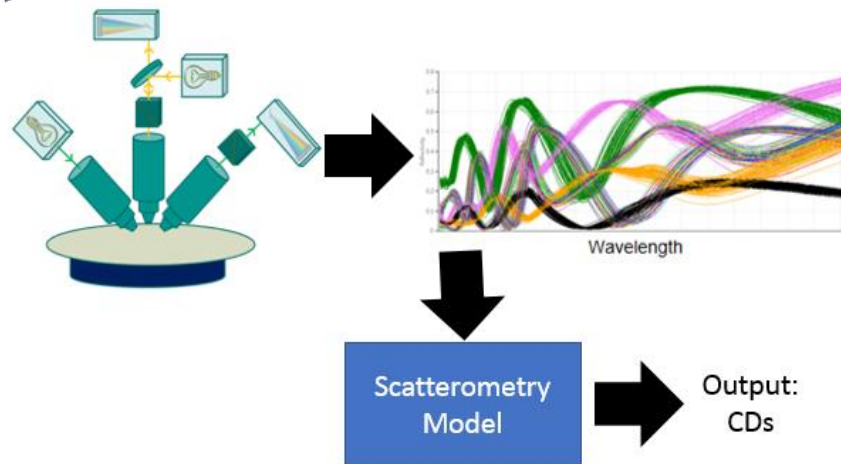


Figure 2. The schematics of scatterometry metrology. Multiple channels of spectra are collected and interpreted with the model which mimics the actual structures. The profile information can be extracted by matching the calculated spectra from model with measured spectra.

2.2 Critical Dimension Scanning Electron Microscope (CDSEM)

CDSEM is a popular in-line metrology, which provides information from the surface of a structure in top-down view. CDSEM provides linewidth (also referred to as CD) or space information by analyzing the high-resolution SEM images. The drawbacks of CDSEM are: low throughput, small sampling size, limited to top-down image analysis, and damage to photoresist and low-k materials.

2.3 Machine Learning

Machine learning is a popular topic for big data mining, and involves statistics, data analysis, programming algorithms and artificial intelligence. In this section, we will only briefly introduce machine learning methods specifically for scatterometry.

Fig. 3 shows the schematics of machine learning methods for scatterometry. It involves two phases to implement the ML methods for in-line measurement, ML algorithm/model training and in-line measuring. In phase I, a data set needs to be collected, which includes the scatterometry spectra and the reference data corresponding to each set of spectra. This data set is used for training the ML algorithms and for validating the accuracy. Once the ML algorithms achieve acceptable accuracy during the validation, the ML solution is generated and then installed on the tool for further in-line measurement.

Since ML methods do not require the use of a physical model, they can be used to complement scatterometry for those applications that contain non-periodic features [7]. For instance, the random (non-periodic) nature of the defects and surface/line roughness can be better characterized with scatterometry complemented with scatterometry-enabled ML.

3. RESULTS AND ANALYSIS

In this work, we first evaluated the simple conventional scatterometry model which does not include nodule defects, in order to determine the sensitivity of a scatterometry model to the nodules. This is referred to as Model 1. Periodic parameters to approximate the random nodule defects were then added to create Model 2. Finally, a machine learning solution was introduced to support the accurate measurement of the nodule defects. Model 3 is the hybridization of the ML solution with Model 2. Each of these 3 models will be discussed in detail in the following sub-sections.

3.1 Model 1 --- Conventional Scatterometry Model without Including Defects

In order to test the sensitivity of the nodules to scatterometry, a model with no nodules is created. It would follow that if there is sensitivity to the nodules in the spectra, this model would result in inadequate spectral fits. Conversely, if there is no sensitivity to the nodules, the model would be able to achieve good fits.

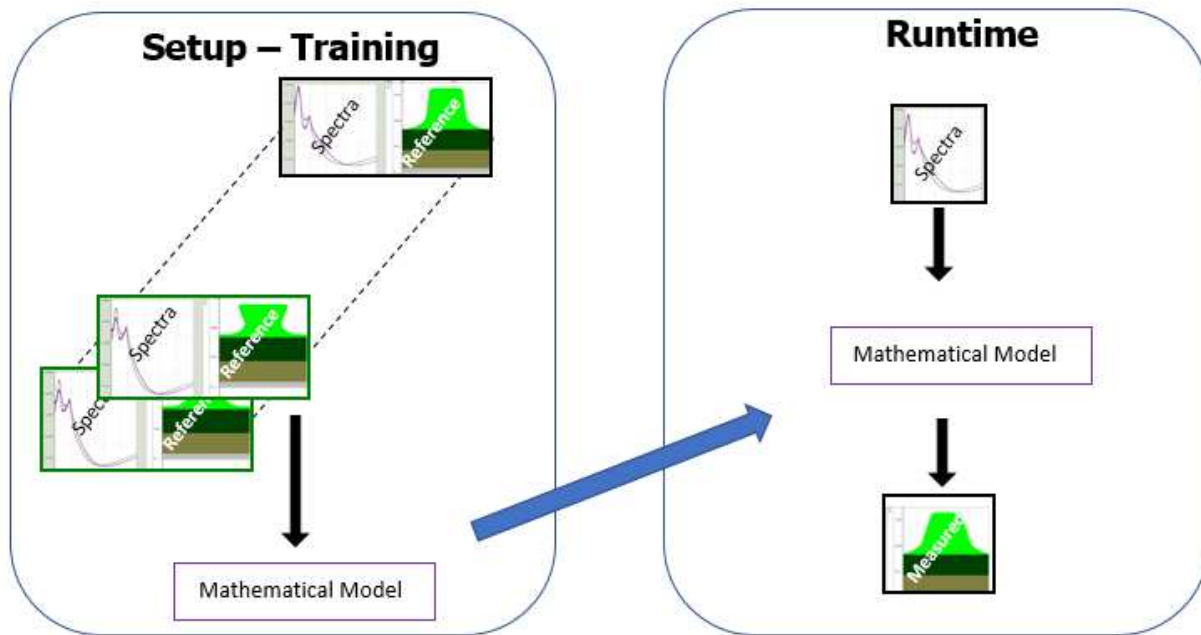


Figure 3: The schematics of machine learning for scatterometry-based applications. A mathematical model, or solution, is created by comparing spectra to reference data in the training step, and this mathematical model is then used in production to directly translate the newly measured spectra to a parameter value.

The structure used in this model is shown in fig. 4(a). The spectral fit corresponding with this model is inadequate, as shown in fig. 4(b). We can see that the Goodness of Fit (GOF) for the low defect density wafer is relatively stable, with values close to 0.9 or greater. However, the GOF for the high defect density wafer varies a lot, from about 0.5 to 0.9. Analysis shows that the dies with low GOF have heavy nodule defects, which suggests that nodule defects have significant effect on the performance of the conventional scatterometry model.

The inadequate fitting of Model 1 drives an improvement by introducing defects into the model. This improved model will be discussed in the next sub-section.

3.2 Model 2 --- Conventional Scatterometry Model with Nodule Defects

As mentioned in the previous section, the random nodule defects cannot be precisely modeled in conventional scatterometry. However, periodic parameters can be used to approximate the SiGe nodule defects [6]. The model is set up with the assumption there is one nodule defect per unit cell, and each nodule bridges the two neighboring dummy gate structures. Fig. 5 shows how the nodule defects are represented. Three parameters are introduced to approximately characterize the nodule defects: These are the nodule width, height and vertical location. The nodule width is the size of

each nodule defect in the direction parallel to the dummy gates from top-down view. The nodule height is the measurement of average vertical thickness of nodule defects. The nodule vertical location describes where the defects between PC gates are located in the direction of wafer normal. It should be emphasized that one of the main goals of this work is to measure the vertical location of nodule defects.

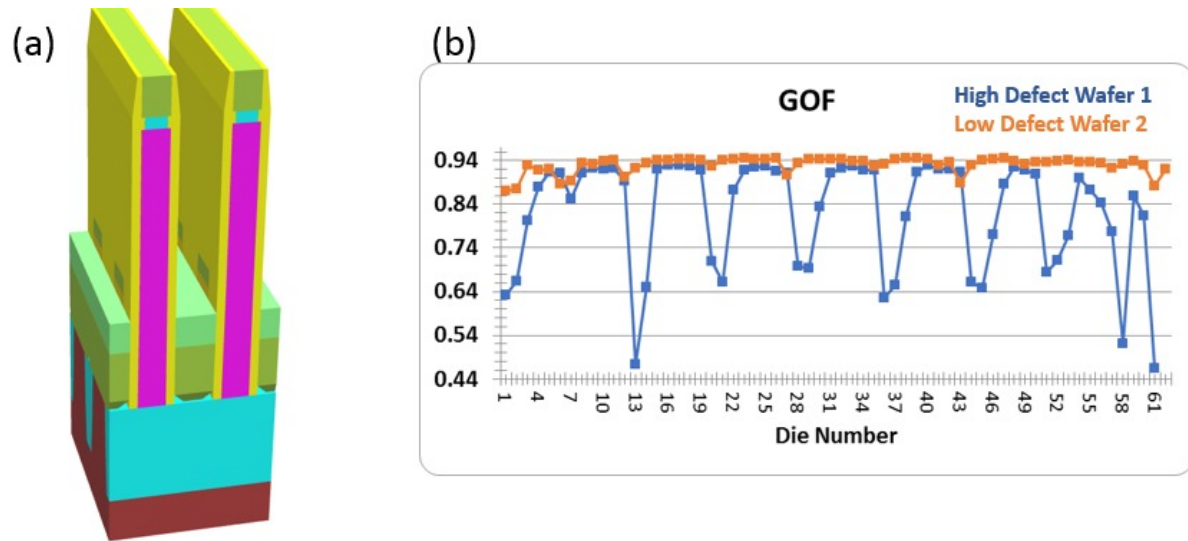


Figure 4. (a) Shows the structure of Model 1, which is a conventional scatterometry model without including nodule defects. (b) Shows that the goodness of fit (GOF) is inadequate and that the scatterometry model is significantly affected by the amount of nodule defects.

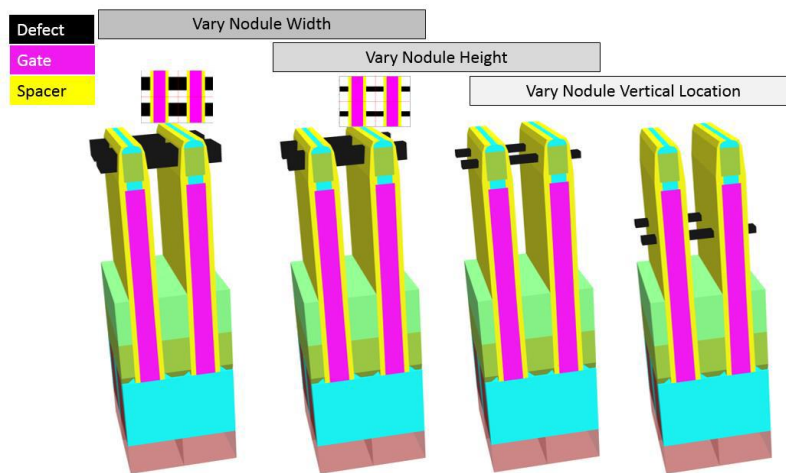


Figure 5. Structure of Model 2. The nodule defects are estimated with periodic parameters, nodule width, nodule height and nodule vertical location.

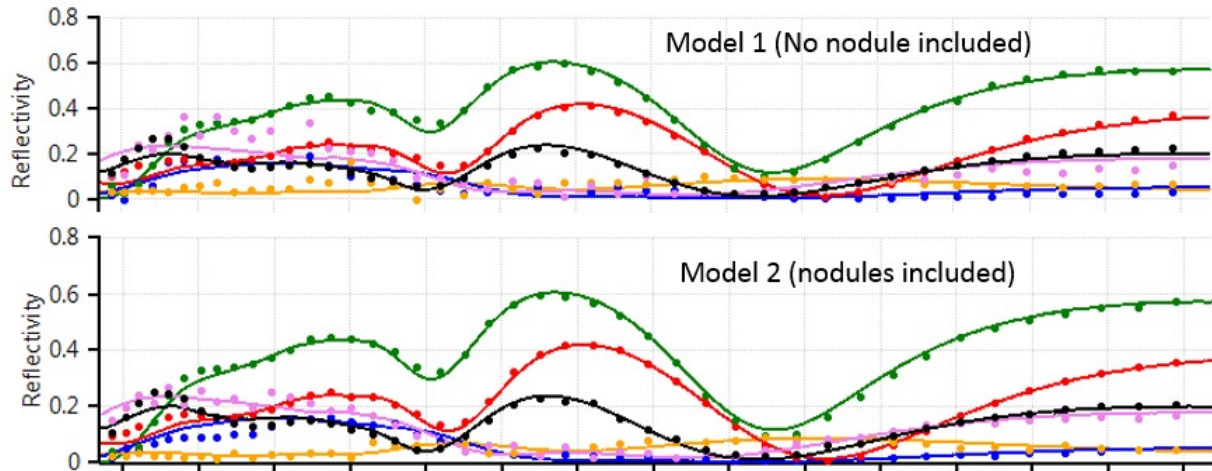


Figure 6. The comparison of GOF between Model 2 and Model 1 is shown here. It indicates that Model 2 provides significantly better fitting than Model 1.

The comparison of GOF between Model 1 and Model 2 is shown in fig. 6. For the same set of spectra collected from the die with moderate nodule defects, the GOF of Model 2 is significantly better than Model 1, which indicates that including nodule defects in the scatterometry model is necessary for good fitting. It also indicates that the random nodule defects can be approximated using periodic parameters in the scatterometry model.

Even though the GOF can be improved by using periodic parameters to estimate nodule defects, the average vertical location of nodule defects extracted from Model 2 remains a challenge due to low sensitivity for this parameter, and therefore this is not sufficient to solve the problem.

3.3 Model 3 --- Hybridization of ML and Model 2

As pointed out in section 3.2, the random nodule defects can be estimated with periodic parameters in scatterometry model. However, the random nodule defects can be further characterized by including a ML component, because it accesses additional information that the scatterometry solution does not.

Machine learning is used to create a link directly between acquired spectra and an external reference. In this work, CDSEM images are used as reference data. CDSEM images were acquired on the same location as the scatterometry measurement and are analyzed offline with an in-house software package to extract nodule defect density and area fraction covered by nodule defects. The nodule defect density and the area fraction covered by nodule defects are referred to each set of spectra from the same die, and then the ML algorithms are trained to analyze and “learn” the reference results. After training, the ML algorithms can assist in the quantification of the nodule defects. The comparison of the ML-based results with CDSEM reference data is shown in fig. 7.

In fig. 7, it shows the nodule defects predicted from ML has accuracy > 95%. The data shown in fig. 7 is for ML validation, which is completely different from ML training data set. In other words, it is considered that the data set for ML validation should be different from the ML training data set. Fig. 7(a) shows the nodule defect density predicted from ML matches the SEM reference results within 95% accuracy, and (b) shows the area fraction covered by nodule defects predicted from ML matches the SEM reference results with a better accuracy, 98%. The excellent accuracy demonstrates that the ML methods can enable a reliable measurement of the density of the random nodule defects. Model 3 is a hybridization of the scatterometry-based ML solution and the conventional scatterometry Model 2, enabling the measurement of the area fraction covered by nodule defects.

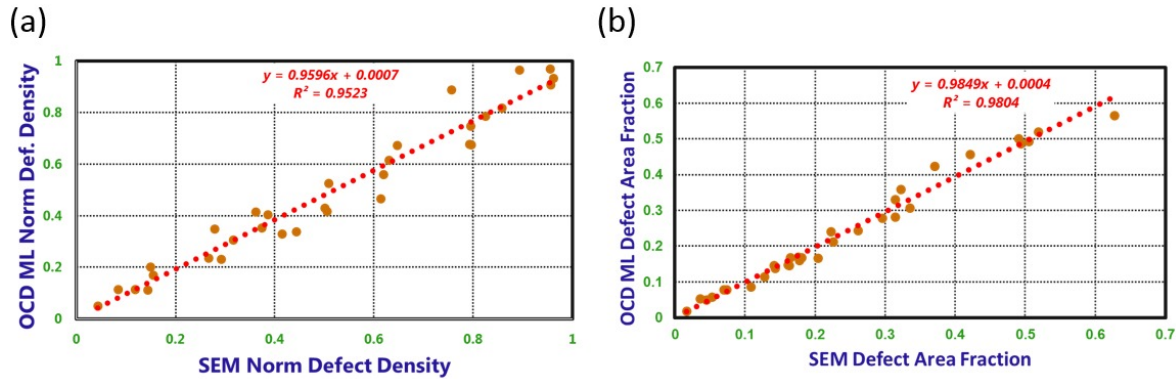


Figure 7. (a) Shows the nodule defect density predicted from ML matches the results from SEM very well with an accuracy of 95%. (b) Shows the area fraction covered by nodule defects as measured by ML also matches SEM results with an accuracy of 98%.

One of the main goals of this work is to reveal the information about vertical location of nodule defects. By incorporating ML and hybridizing with a conventional scatterometry model, this reduces the number of degrees of freedom that the conventional model must solve, and enables us to solve additional parameters which are of lower sensitivity, such as the vertical location of nodule defects. Fig. 8 shows the comparison of the vertical location parameter between Model 2 and Model 3. The wafer maps shown in fig. 8 are from the POR wafer, which has fewer nodule defects than the second wafer. The left wafer map is derived from Model 2, and the right one is from Model 3. If we compare these two wafer maps, the pattern of the wafer maps significantly improves by introducing hybridization of ML with Model 2. The wafer map on the right-hand side, from Model 3, has better radial symmetry, which matches the expectation from a process point of view. The average vertical location of nodule defects from Model 3 is compared with cross-sectional SEM (XSEM) data in order to confirm the results.

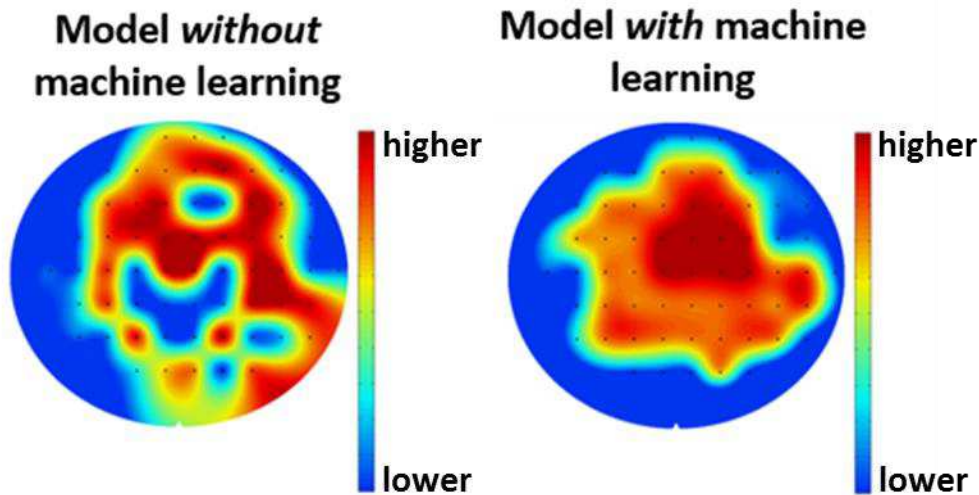


Figure 8. Wafer maps of the vertical location of nodule defects for POR wafer are shown in this figure. The left wafer map is from Model 2, and the right wafer map is from Model 3, which is the hybridization of Model 2 with ML.

The table in fig. 9 summarizes the comparison of vertical location between XSEM, Model 2 and Model 3, for three dies.

This can be at most a qualitative comparison, as the number of cross-sectional images required for a rigorous statistical comparison would require significantly more resources than were available for this project.

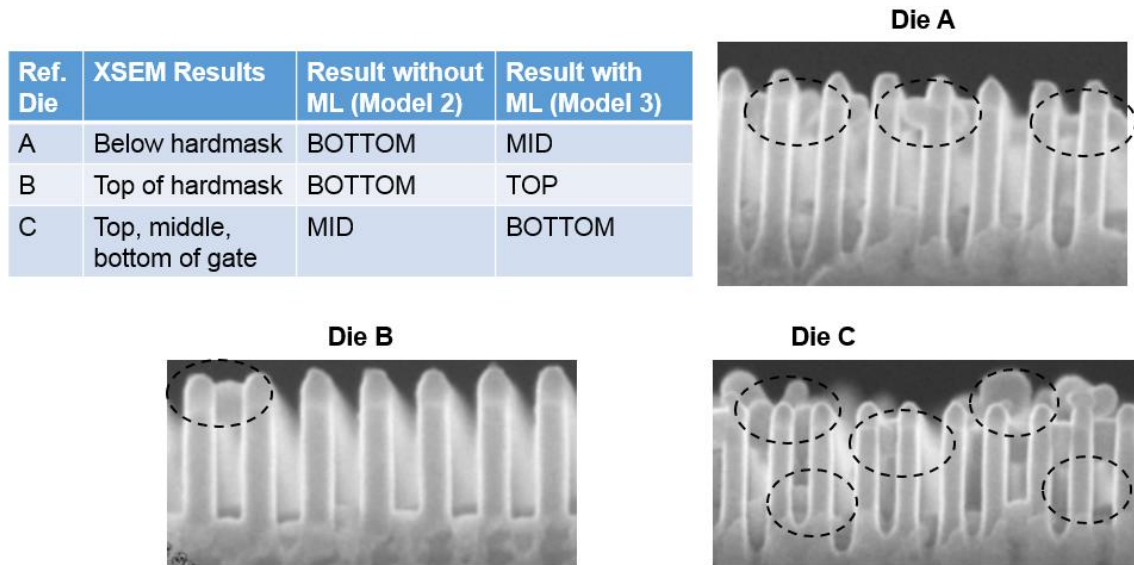


Figure 9. The results about the vertical location from both Model 2 and Model 3 are qualitatively compared with the observation from cross-sectional SEM (XSEM) data. Model 3 appears to follow the trend as shown in XSEM data better than Model 2.

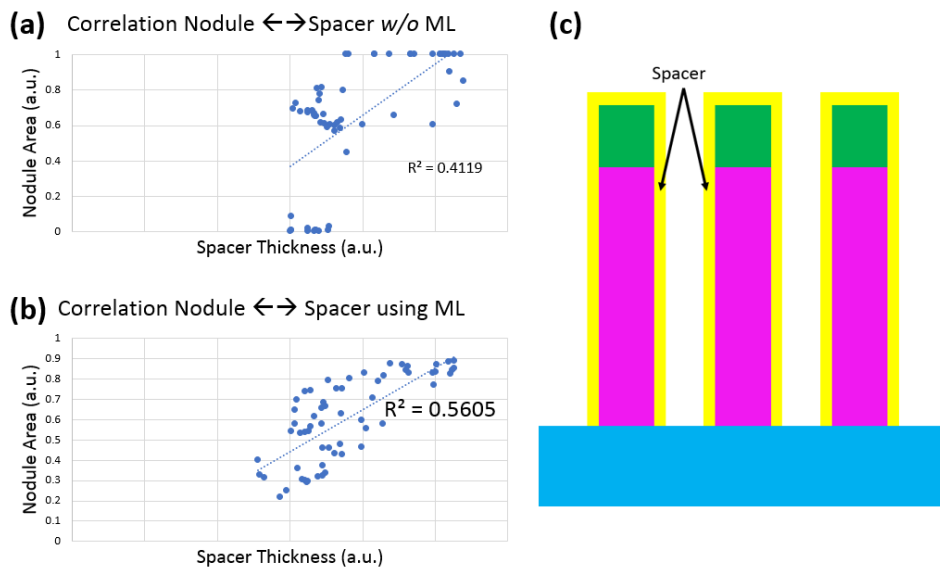


Figure 10. (a) Shows the correlation analysis results between nodule defects and spacer thickness from Model 2 (no ML). (b) Shows the correlation analysis results from Model 3, with hybridization of ML and Model 2. The correlation between nodule defect and spacer thickness in (b) is more obvious than (a). The cartoon in (c) is used to explain in the text the correlation between nodule defects and spacer thickness.

The XSEM images for the selected 3 dies are also shown in fig. 9, as labeled. For Die A and B, Model 3 provides a much better match to the reference than Model 2. The XSEM data shows that the nodules are primarily located near the hardmask

atop the dummy gate. Model 2 is reporting that the nodules are at the bottom of the structure, while Model 3 reports that the nodules are at the middle (Die A) and the top (Die B) of the structure, much closer to what is reported in the XSEM. For Die C, it is harder to discern, as the XSEM shows nodules along the top, middle, and bottom of the gate, while Model 2 and Model 3 are only able to output one expected location for the nodules.

Since Model 3 has promising results for both structural parameters and nodule defects, it enables correlation analysis between the defects and the structural parameters. Fig. 10 shows the correlation analysis results between nodule defects and spacer thickness. Fig. 10(a) shows the correlation results from Model 2, and (b) shows the results from Model 3. Both (a) and (b) shows that the nodule defect increases with the thickness of spacer, but the hybridization of the model shows a much stronger correlation, which is consistent with the process expectation. In fig. 10(c), the schematics of the cross-gate structure is provided, in order to help more clearly understand why the amount of nodule defects increase with spacer thickness. Two things may happen when spacer thickness increases: the open space between the dummy gates becomes smaller as spacer thickness increases, and the roughness of spacers may increase with thickness. As spacer thickness increases, the opening space gets smaller, which makes it more difficult for the precursor gas of the EPI process to reach the bottom of the gate. This increases the chances of growing non-selective nodule defects. The increase in spacer roughness can also introduce more nucleation sites for nodule defects to grow.

In this section, all of the 3 models are investigated and evaluated. Model 1, because it does not include nodule defects, cannot provide a correlation that depends on the nodule defects. Model 2, using periodic parameters to estimate random defects in model, provides reasonable fit for dies or wafers with or without nodule defects. Model 3, hybridizing ML with Model 2, can provide the measurement of vertical location of nodule defects, and of correlation between nodule defects and structural parameters.

4. SUMMARY

In this work, we develop a novel in-line characterization technique for SiGe nodule defects which has high throughput and is non-destructive. The technique is scatterometry-based, and employs sophisticated ML algorithms. It is demonstrated that hybridizing the ML methods with a conventional scatterometry model allows us to measure the vertical location of nodule defects, which is an important parameter that affects device yield. For example, the nodule defects at gate middle or bottom will block the contact of tungsten to S/D epi. Our new technique also reveals the correlation between nodule defects and spacer thickness. This information is useful for the EPI process engineer to optimize the EPI process.

ACKNOWLEDGEMENTS

The authors would like to acknowledge Tom Gow Jr & Mukesh Khare from IBM for management support.

REFERENCES

1. I. Lauer et al., "Si nanowire CMOS fabricated with minimal deviation from RMG FinFET technology showing record performance," 2015 Symposium on VLSI Technology (VLSI Technology), Kyoto, 2015, pp. T140-T141.
2. N. Loubet et al., "Stacked nanosheet gate-all-around transistor to enable scaling beyond FinFET", 2017 Symposium on VLSI Technology, Kyoto, 2017, pp. T230-T231.
3. G. R. Muthinti, "Mueller based scatterometry measurement of nanoscale structures with anisotropic in-plane Optical properties", Proc. SPIE 8681, Metrology, Inspection, and Process Control for Microlithography XXVII, 86810M (2013)
4. Muthinti, R., Loubet, N., et al. "Advanced in-line Optical metrology of sub-10nm structures for gate all around devices (GAA)" in *Metrology, Inspection, and Process Control for Microlithography XXX*, edited by Martha I. Sanchez, Proceedings of SPIE Vol. 9778 (SPIE, Bellingham, WA 2016) pp. 977810-1 – 977810-8.
5. Sendelbach, M., Sarig, N, et al. "Impact of shrinking measurement error budgets on qualification metrology sampling and cost" in *Metrology, Inspection, and Process Control for Microlithography XXVIII*, 90501M (2014).

6. Dexin Kong, Liying Jiang, Jeff Drucker, “Interpreting plasmonic response of epitaxial Ag/Si(100) island ensembles”, *J. Appl. Phys.* 118, 213103 (2015).
7. Robin Chao, Chi-Chun Liu, et al., “Scatterometry-based Defect Detection for DSA In-line Process Control”, in *Metrology, Inspection, and Process Control for Microlithography XXIX*, edited by Jason P. Cain, Proc. SPIE Vol. 9424, pp. 942419-1 – 942419-17.